A Vision-Driven Model Based on Cognitive Heuristics for Simulating Subgroup Behaviors During Evacuation

Wenhan Wu, Wenfeng Yi, Xiaolu Wang, and Xiaoping Zheng

***Abstract*— Due to the universal existence of human subgroups in reality, an increasing number of studies have incorporated them into the modeling process of crowd evacuation. However, such models seldom explain subgroup behaviors from the aspect of what individuals see and how they respond to visual input. Here, we propose a vision-driven model based on cognitive heuristics, in which the mechanisms of avoidance with the environment and attraction to other members within the field of view are explicitly clarified. Numerical simulations demonstrate that various spatial characteristics of subgroup members can be effectively represented by this model, and both the intensity and heterogeneity of spatial cohesion have significant impacts on subgroup evacuation. By comparing with an empirical study, the reproducibility of our model has been validated in terms of the temporal and spatial dimensions. This model produces more natural and realistic subgroup behaviors in multiple interaction contexts than existing models, and also quantitatively exhibits the superiority in reproduction effects. Overall, this work provides an interpretable mathematical framework for modeling subgroups from the perspective of visual perception.**

***Index Terms*— Subgroup behaviors, evacuation dynamics, cognitive heuristics, decision making, visual information.**

I. Introduction

WITH the increasing frequency of human activities in public places, crowd analysis and modeling has been attracting considerable interest as an important research field [1], [2]. Related studies such as crowd counting [3], [4], behavior detection [5], [6], trajectory prediction [7], and scene segmentation [8] have achieved important breakthroughs, which provide valuable insights into the management and control of crowds. In recent years, the rapid development of computer simulations has given rise to a large number of crowd evacuation models [9], [10], which replicate a rich diversity of self-organization phenomena and contribute to the understanding of human collective behaviors [11]. Due to the fact that human crowds are not entirely composed of isolated individuals in reality [12], subgroups (i.e., a collective term for social groups, pedestrian groups, small groups, etc. in other literature) are gradually considered as a crucial topic in the modeling process [13]. However, it is by no means an easy task for translating the behavioral characteristics of subgroups into explicit mathematical representations, and therefore constructing relevant models that describe subgroup behaviors during evacuation is an important research undertaking.

As one of the most classical models inspired by Newtonian mechanics, the social force model (SFM) [14] simulates the escape behavior of pedestrians via the combination of a self-driven force, an interaction force with other individuals, and an interaction force with walls or obstacles. This model is convenient to expand and modify by incorporating specific forces to realize the coordination movement of subgroup members. Li et al. [15] integrated the attractive force of subgroups into the SFM and grouped the crowd based on grid density and social relationship to reproduce the actual motion of crowd evacuation. Zhang et al. [16] developed a two-layer SFM considering the interaction between leaders and members, and experimental results successfully reflected subgroup behaviors in earthquake evacuation. Xie et al. [17] improved the SFM by introducing the Lennard-Jones potential that characterizes the long-range attraction and short-range repulsion among subgroup members, relevant simulations indicated that the subgroup effect promotes the overall evacuation time. Nevertheless, we notice that the above models have several core issues: First, the "bird's-eye perspective" assumes that pedestrians have access to information about the environment outside their field of view, which is contrary to human physiological properties in real situations [18]. Second, pedestrians can react to the motion states of surrounding neighbors, but certain social information (e.g., velocity vectors) has not been explicitly encoded in their visual input [19]. These issues have led to our doubts about the plausibility of evacuation simulations associated with subgroups. Hence, we believe it is necessary to gain a deeper understanding of how individuals process the acquired sensory information and develop a bottom-up subgroup model to reproduce phenomena and behaviors more in accordance with empirical observations.

For a wide range of biological systems such as insects [20], fish [21], [22], and birds [23], [24], vision has been confirmed by considerable studies as a key element in the emergence of collective behavior. However, the information processing [25] (e.g., neural mechanisms, encoding styles) and spatio-temporal

Manuscript received 23 June 2023; revised 2 April 2024; accepted 24 June 2024. This work was supported in part by the National Key Research and Development Program of China under Grant 2021YFB3301100 and in part by the National Major Scientific Research Instrument Development Project under Grant 61927804. The Associate Editor for this article was J. Alvarez. *(Corresponding author: Xiaoping Zheng.)*

The authors are with the Department of Automation, Beijing National Research Center for Information Science and Technology, Tsinghua University, Beijing 100084, China (e-mail: wwh19@mails.tsinghua.edu.cn; yiwf22@mails.tsinghua.edu.cn; wangxlu@mail.tsinghua.edu.cn; asean@mail.tsinghua.edu.cn).

Digital Object Identifier 10.1109/TITS.2024.3421626

patterns [26] (e.g., polarized rotations, crystal-like configurations) exhibited by animals differ significantly from those of humans, making it difficult for relevant findings to be referred for modeling crowd motion in social systems. To our knowledge, several studies have attempted to integrate vision into force-based crowd models. Helbing et al. [27] incorporated the anisotropic features of pedestrian interaction into the SFM, for the purpose of simulating crowds in normal and evacuation situations more realistically. Moussaïd et al. [28] established a vision-based mechanistic model to reproduce the observed phenomena of crowd disasters at extreme densities, in which the desired speeds and desired directions of pedestrians were determined by heuristic rules. Ma et al. [29] extended the SFM from the perspective of view radius and found that the effect of guides on crowd evacuation is associated with the neighbor density within the field of view. Meng et al. [30] improved the SFM by combining visibility distance and herding behavior to explore emergency evacuation under the view-limited conditions. Yi et al. [31] developed an extended queuing model considering visual and morality, and numerical simulations denoted that it successfully predicts the "detour" phenomenon in crowd evacuation. Despite that vision has been more or less covered in these studies, however, the vast majority of them cannot fully address the core issues mentioned previously. More critically, subgroup factors are also largely ignored in the modeling process based on sensory information, resulting in the lack of evacuation models that utilize visual perception to drive subgroup movement.

In this paper, we propose a vision-driven model based on cognitive heuristics for simulating subgroup behaviors during evacuation. Our key contribution is to explicitly define two cognitive heuristics for subgroup movement from the viewpoint of individual response to visual information. Here, the first heuristic "A subgroup member chooses a trade-off between the individual desired direction and the subgroup desired direction" determines the mathematical form of the desired direction, and the second heuristic "A subgroup member adjusts the desired speed in avoiding collisions with obstacles and avoiding separation from the subgroup" produces the functional expression of the desired speed. These two cognitive heuristics are simultaneously integrated into the equations of motion to describe the coordination movement of subgroup members. Numerical simulations show that the critical distance of the local interaction range can be regarded as a good representation of spatial cohesion, whose intensity and heterogeneity both have non-negligible effects on subgroup evacuation. According to an empirical study on how subgroups affect crowd evacuation, the reproducibility of our model has been validated from the temporal and spatial dimensions. Compared with existing models, our model produces more natural and realistic subgroup behaviors and exhibits the superiority in reproduction effects. In conclusion, this work makes valuable contributions to better understanding the behavioral characteristics of subgroups during evacuation.

The rest of this paper is organized as follows. In Section II, two cognitive heuristics are defined to construct a vision-driven model for simulating subgroup behaviors. Section III presents a series of numerical simulations and corresponding analytical explanations. Finally, relevant conclusions and future prospects are summarized in Section IV.

II. Mathematical Model

A. Description of Visual Information

Vision, as one of the most important human senses for capturing external information, has been considered as the primary interaction mechanism of collective behavior. In general, when pedestrian i attempts to reach the destination point O_i, whose visual projection field S_i^{vis} can be formally characterized as a sector area with a maximum horizon distance $d_{\max}$, ranging to the left and to the right by φ degree with respect to the line of sight $\mathbf{h_i}$, where $\mathbf{h_i}$ is assumed to coincide with the actual movement direction [32]. The information within the visual projection field S_i^{vis} is mainly reflected in two aspects: First, the highest priority for a pedestrian interacting with other individuals and environments is to avoid collisions, and this is regulated by neural mechanisms at the retinal and brain levels [33], [34]. Second, the state changes of surrounding neighbors may also significantly affect the encoding of visual information [19], leading to the alteration in pedestrian perception and behavior. As a result, the motion response of pedestrian i to visual information will trigger the dynamic updates of velocity $\mathbf{v}_i(t)$ and position $\mathbf{x}_i(t)$.

B. Cognitive Heuristics for Subgroup Movement

Here, we introduce two cognitive heuristics for subgroup movement [35], and such a simple and fast method can be used to describe the decision making in individual interactions. The first heuristic determines the desired direction during the escape process. Empirical evidence points out that pedestrians prefer to reach their destination by an unobstructed path, but without deviating too much from the straight path by detours [36]. This fact indicates that a subgroup member generally chooses the most direct path to escape when other individuals and obstacles are considered. Here, $d(\theta)$ is measured as a squared function of the distance to the destination at directional angle $\theta \in [-\varphi, \varphi]$:

$$d(\theta) = d_{\max}^2 + f(\theta)^2 - 2d_{\max} f(\theta)\cos(\theta_0 - \theta) \tag{1}$$

where $f(\theta)$ is the expected distance to the first collision when subgroup member i moves into directional angle θ at speed v_i^{avs}, and θ_0 represents the directional angle of the destination point O_i. The individual desired directional angle $\theta_i^{ind} = \arg\min d(\theta)$ is derived by minimizing the function $d(\theta)$, whereby the corresponding normalized vector $\mathbf{e}_i^{ind}$ can be written as:

$$\mathbf{e}_i^{ind} = \left[\cos(\theta_i^{ind}), \sin(\theta_i^{ind})\right] \tag{2}$$

Besides, it has been reported that individuals tend to maintain aggregation with their surrounding neighbors within a local interaction range [37], which allows them to move in the form of "cliques" and avoid frequent disintegrations. In this case, a subgroup member is expected to be attracted by other members in the field of view [38] until entering a certain local

interaction range, which gives rise to the expression of the subgroup desired direction $\mathbf{e}_i^{sub}$:

$$\mathbf{e}_i^{sub} = \frac{\langle \mathbf{x}_q \rangle_{q \in S_i^{vis}} - \mathbf{x}_i}{\left\| \langle \mathbf{x}_q \rangle_{q \in S_i^{vis}} - \mathbf{x}_i \right\|} \tag{3}$$

where $\mathbf{x}_q$ are the positions of other members q within the visual projection field S_i^{vis}. Therefore, the first heuristic is defined as "A subgroup member chooses a trade-off between the individual desired direction and the subgroup desired direction". This results in the desired direction of subgroup member i as below:

$$\mathbf{e}_i^{des} = \frac{(1-\alpha_i)\mathbf{e}_i^{ind} + \alpha_i \mathbf{e}_i^{sub}}{\|(1-\alpha_i)\mathbf{e}_i^{ind} + \alpha_i \mathbf{e}_i^{sub}\|} \tag{4}$$

Here, the follow willingness coefficient is defined as $\alpha_i = g(d_{ic} - d_i^*)/(d_{\max} - d_i^*)$, where $d_{ic} = \|\langle \mathbf{x}_q \rangle_{q \in S_i^{vis}} - \mathbf{x}_i\|$ is the distance from subgroup member i to the centroid of other members within the visual projection field S_i^{vis}, and $d_i^* (< d_{\max})$ denotes a critical distance of the local interaction range to avoid separation from the subgroup, with a smaller value reflecting a stronger spatial cohesion. Besides, $g(x)$ is zero if $x < 0$, otherwise it equals the argument x.

The second heuristic is concerned with the formation of the desired speed. On the one hand, pedestrians attempt to avoid collisions by maintaining a certain physical space when encountering unexpected obstacles during the escape process. This implies that a subgroup member will keep a safe distance from the nearest obstacle in the movement direction, which allows a time period τ_i to stop before the collision occurs. Assuming that d_i^h is the distance to the first potential obstacle along the desired direction $\mathbf{e}_i^{des}$, the desired speed v_i^{avc} for avoiding collisions is calculated as follows:

$$v_i^{avc} = \frac{d_i^h}{\tau_i} \tag{5}$$

On the other hand, individuals strive to avoid separation from the subgroup to which they belong to maintain aggregation [39]. It means that a subgroup member will generate accelerated behavior to avoid falling behind if he or she is apparently far away from other members in the field of view. This can be expressed as the desired speed v_i^{avs} for avoiding separation:

$$v_i^{avs} = (1-\alpha_i)v_i^0 + \alpha_i v_i^{\max} \tag{6}$$

where v_i^0 and $v_i^{\max}$ represent the initial and maximum desired speeds of subgroup member i, respectively. That is, a farther distance from this member to the centroid of other members in the field of view will induce the willingness to follow them at a faster speed.

From this, the second heuristic is defined as "A subgroup member adjusts the desired speed in avoiding collisions with obstacles and avoiding separation from the subgroup". The desired speed of subgroup member i is therefore given by:

$$v_i^{des} = \min\left(v_i^{avc}, v_i^{avs}\right) \tag{7}$$

Based on these two cognitive heuristics, the desired speed v_i^{des} located in the desired direction $\mathbf{e}_i^{des}$ constitutes the desired velocity $\mathbf{v}_i^{des}$ of subgroup member i. For further aspects of the above definitions see the illustration in Fig. 1.

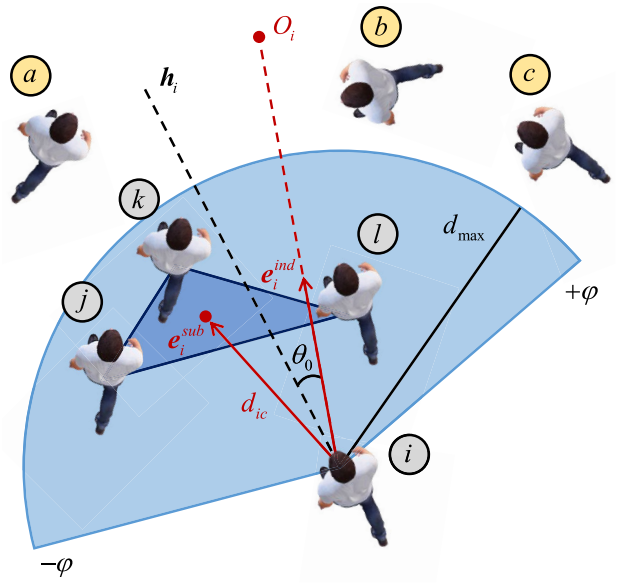

Fig. 1. Illustration of the definitions in cognitive heuristics. A subgroup member i attempts to reach the destination point O_i when facing other members j, k, l within the same subgroup and external pedestrians a, b, c.

C. Equations of Motion for Subgroup Members

The above-mentioned two cognitive heuristics for subgroup movement are integrated into the equations of motion, which primarily affects the desired velocity in the self-driven force. Here, the position $\mathbf{x}_i(t)$ of subgroup member i is updated by the following equation:

$$\frac{d\mathbf{x}_i(t)}{dt} = \mathbf{v}_i(t) \tag{8}$$

where the temporal variation of velocity $\mathbf{v}_i(t)$ is characterized by the nonlinear coupling Langevin equation as below:

$$m_i \frac{d\mathbf{v}_i(t)}{dt} = \mathbf{f}_{id} + \sum_{j(\neq i)} \mathbf{f}_{ij} + \sum_W \mathbf{f}_{iW} \tag{9}$$

in which the velocity changes with the combined effect of the three forces on the right side of the above equation.

First, the self-driven force $\mathbf{f}_{id}$ describes that individual acceleration is determined by the perception mechanism of visual information, which is expressed as follows:

$$\mathbf{f}_{id} = m_i \frac{\mathbf{v}_i^{des}(t) - \mathbf{v}_i(t)}{\tau_i} \tag{10}$$

where subgroup member i of mass m_i tends to move with a desired velocity $\mathbf{v}_i^{des}(t)$, whereby adapting his or her actual velocity $\mathbf{v}_i(t)$ within a characteristic time τ_i.

Second, it is also necessary to consider unintentional collisions due to body extrusion at extreme densities, and the physical contact force $\mathbf{f}_{ij}$ with other individuals is given by:

$$\mathbf{f}_{ij} = kg(r_{ij} - d_{ij})\mathbf{n}_{ij} \tag{11}$$

where k is a body elasticity coefficient, $\mathbf{n}_{ij}$ is the normalized vector pointing from individual j to i, r_{ij} indicates the sum

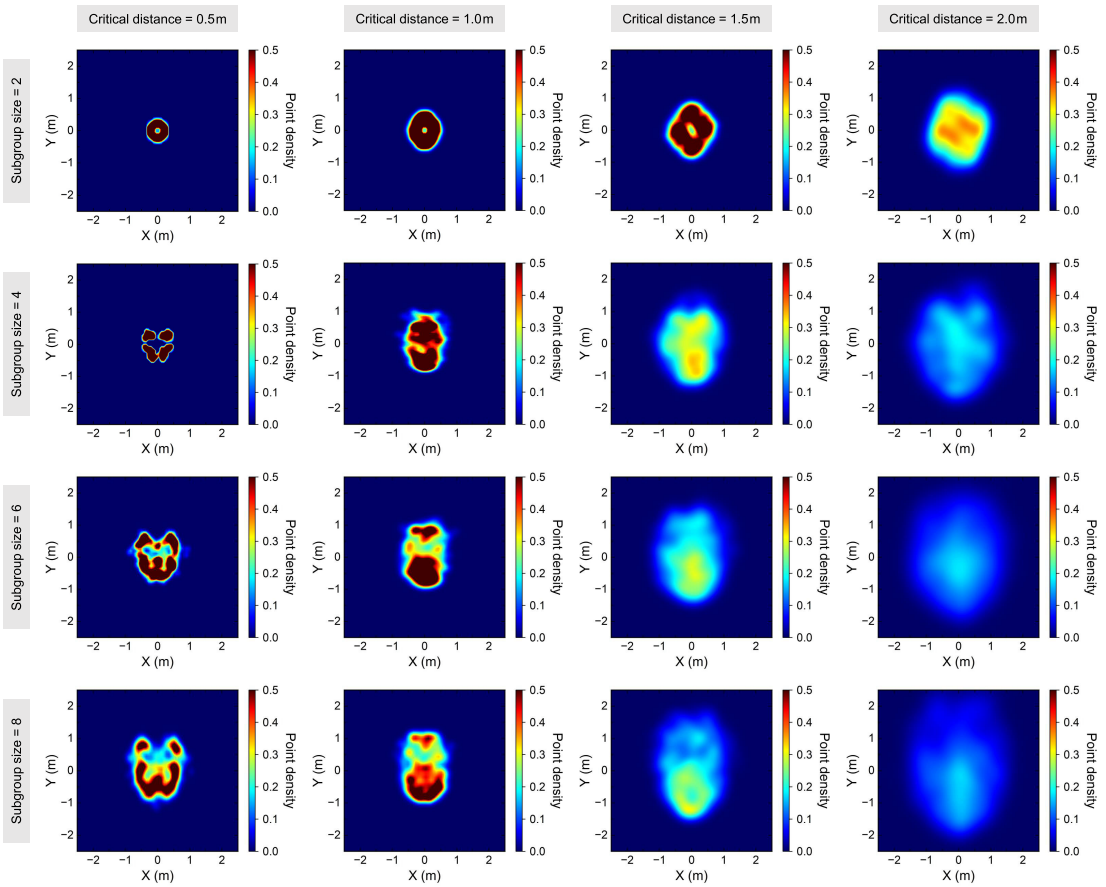

Fig. 2. Point density distributions of spatial positions for subgroup members when the steady state of motion is guaranteed to be reached. The vertical direction indicates different subgroup sizes, and the horizontal direction denotes various critical distances. The color coding represents the specific value of the point density.

TABLE I
PARAMETER SETTINGS OF THE PROPOSED MODEL

Symbol	Description	Value
φ	Vision angle (half-side)	$90°$
$d_{\max}$	Maximum horizon distance	$10\,m$
v_i^0	Initial desired speed	$1\,ms^{-1}$
$v_i^{\max}$	Maximum desired speed	$5\,ms^{-1}$
m_i	Pedestrian mass	$60\,kg$
τ_i	Characteristic time	$0.5\,s$
k	Body elasticity coefficient	$5 \cdot 10^3\,kgs^{-2}$

of their radii r_i and r_j, and d_{ij} denotes the distance between their centers of mass.

Third, such unintentional collisions can also be triggered by environments, and the physical contact force $\mathbf{f}_{iW}$ with walls is analogously written as follows:

$$\mathbf{f}_{iW} = kg(r_i - d_{iW})\mathbf{n}_{iW} \tag{12}$$

where d_{iW} represents the distance from the center of mass of subgroup member i to wall W, and $\mathbf{n}_{iW}$ means the normalized vector perpendicular to it. Note that $\mathbf{f}_{ij}$ and $\mathbf{f}_{iW}$ are nonzero only at extreme densities, whereas they have no effect under normal density conditions.

D. Parameter Settings of the Proposed Model

For parameter settings of the proposed model, whose symbols, descriptions, and values are listed in Table I. The values of vision angle (half-side) φ, maximum horizon distance $d_{\max}$, initial desired speed v_i^0, maximum desired speed $v_i^{\max}$, pedestrian mass m_i, characteristic time τ_i, and body elasticity coefficient k are referred to related literature [14], [28]. The body of pedestrians on the horizontal plane is characterized as a circle with radius r_i, which is assumed as $r_i = l_i/10$ proportional to the height $l_i \in [1.62m, 1.89m]$ of participants from an empirical study [40] in Section III-C, while it is fixed as $r_i = 0.2m$ in other simulations. In addition, the values of subgroup size n_g and critical distance d_i^* not included in Table I are given specifically in subsequent sections.

III. NUMERICAL SIMULATIONS

A. Spatial Characteristics at Different Critical Distances

Our goal is first to explore the spatial characteristics of subgroup members at different critical distances. Under the conditions of critical distance $d_i^* = 0.5m$, $1.0m$, $1.5m$, and $2.0m$, the motion processes of subgroups with size $n_g = 2$, 4, 6, and 8 are simulated in an unbounded scenario. We conduct 100 numerical simulations for each case to obtain the statistically significant position distributions, and the relative positions among members are recorded when the steady state of motion is guaranteed to be reached. Fig. 2 displays the point

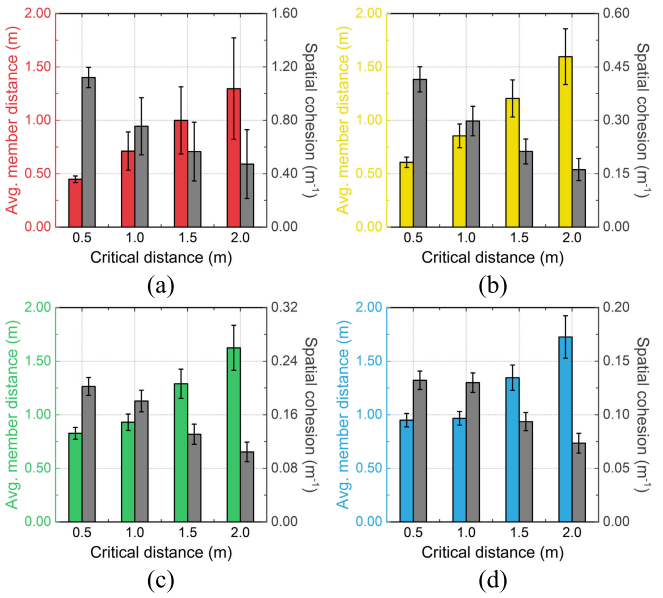

Fig. 3. Bar charts of the average member distance and the spatial cohesion at different critical distances. (a) $n_g = 2$. (b) $n_g = 4$. (c) $n_g = 6$. (d) $n_g = 8$. The top line and whisker represent the mean value and standard deviation, respectively.

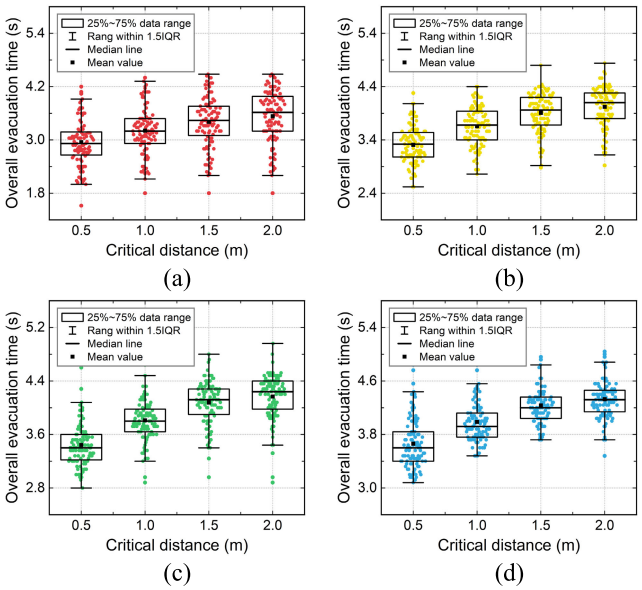

Fig. 4. Box plots of the overall evacuation time at different critical distances. (a) $n_g = 2$. (b) $n_g = 4$. (c) $n_g = 6$. (d) $n_g = 8$. The box indicates the data between the first and third quartiles, the whisker denotes the data within 1.5 times the interquartile range (IQR), and the central thick line and solid block represent the median line and mean value, respectively.

density distributions of spatial positions for subgroup members, where the color coding represents the specific value of the point density. From the vertical direction, it is an obvious fact that the growing subgroup size gives rise to the expansion of the distribution area of spatial positions. From the horizontal direction, the increase in critical distance causes the distribution area of spatial positions to diffuse outward from the center, accompanied by a uniform decrease in the point density. It is worth noting that different critical distances may induce differentiated patterns of subgroup organization. At a small critical distance ($d_i^* = 0.5m$), subgroup members often form very close "cliques" to move, which makes the point density distribution distinctly characteristic. When the critical distance reaches moderate levels ($d_i^* = 1.0m$ and $1.5m$), the point densities are relatively higher in the anterior small area and the posterior large area within the distribution area, which exactly corresponds to the asymmetric leader-follower structure in biological groups [41]. With the critical distance increasing further ($d_i^* = 2.0m$), subgroup members are more loosely distributed and it is difficult to present visually evident spatial structures. These phenomena preliminarily demonstrate that the critical distance can determine the spatial characteristics of subgroup members during evacuation, which is crucial for explaining the formation of their relative positions.

To quantitatively analyze the impact of critical distance on the spatial characteristics of subgroup members, two evaluation metrics are proposed for our analysis. One is the average member distance $\bar{d}_g$, measured as the average of the relative distances between all pairs of members within subgroup g, which is given by the following equation:

$$\bar{d}_g = \frac{1}{n_g(n_g-1)} \sum_{i,j \in g} d_{ij} \tag{13}$$

The other is the spatial cohesion c_g, which can be defined as the reciprocal of the product of n_g and $\bar{d}_g$ due to that a smaller

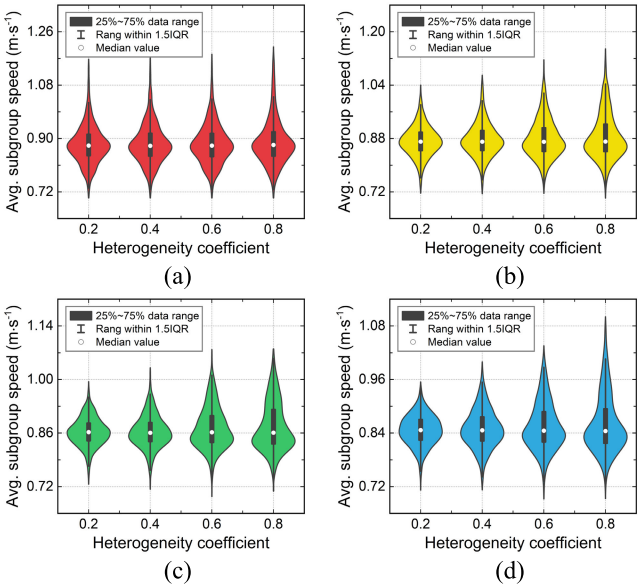

Fig. 5. Violin plots of the average subgroup speed at different values of the heterogeneity coefficient. (a) $n_g = 2$. (b) $n_g = 4$. (c) $n_g = 6$. (d) $n_g = 8$. The box indicates the data between the first and third quartiles, the whisker denotes the data within 1.5 times the interquartile range (IQR), and the central hollow circle represents the median value.

number of members and a shorter average member distance generally correspond to a stronger spatial cohesion:

$$c_g = \frac{1}{n_g \bar{d}_g} = \frac{n_g - 1}{\sum\limits_{i,j \in g} d_{ij}} \tag{14}$$

In this case, the above spatial characteristics of subgroup members are further analyzed by these two evaluation metrics. Fig. 3 shows the bar charts of the average member distance and the spatial cohesion at different critical distances. As the critical distance increases, the overall trends of monotonically increasing average member distance and monotonically

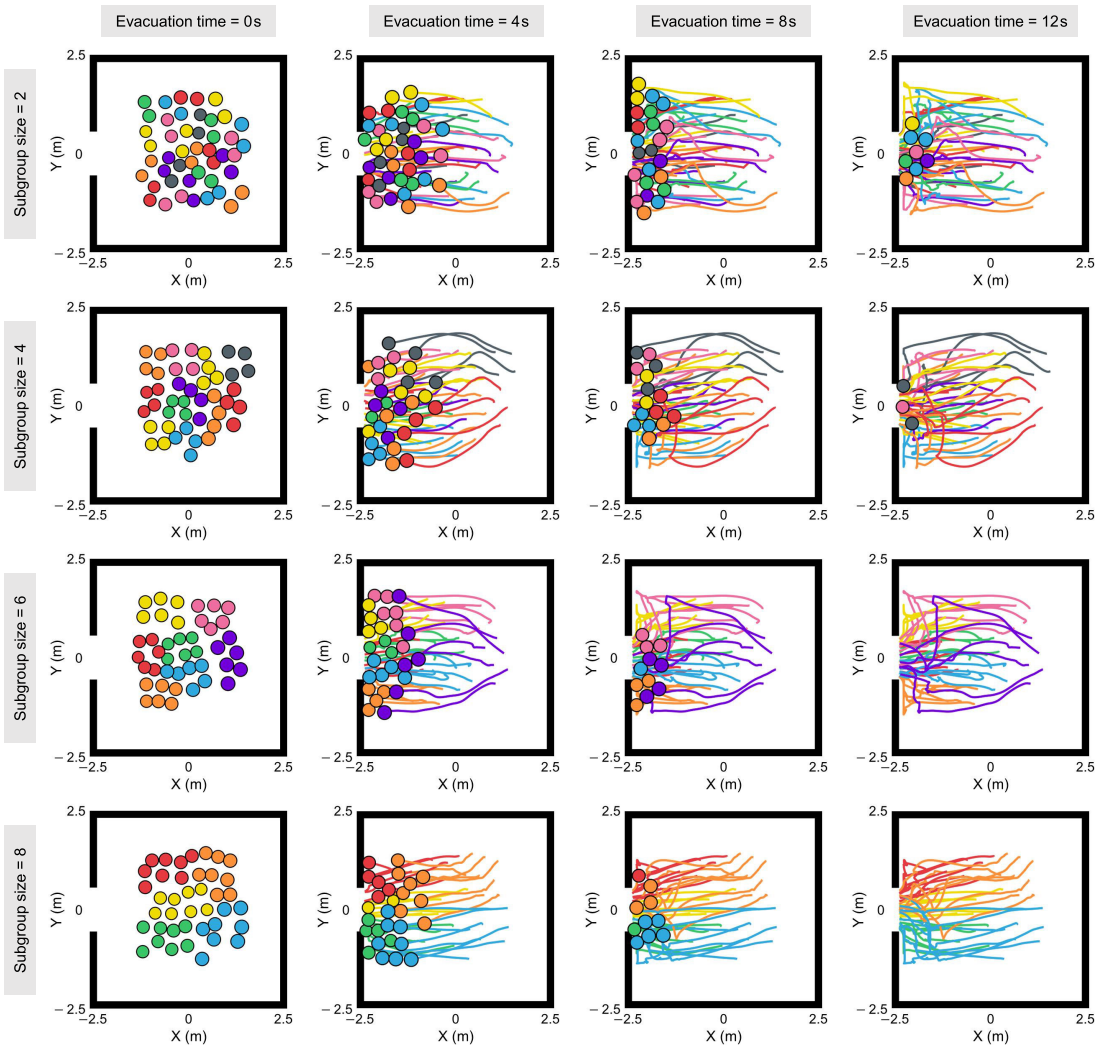

Fig. 6. Simulation snapshots of evacuation processes involving subgroups under experimental conditions. The vertical direction indicates different subgroup sizes, and the horizontal direction denotes various evacuation times. The members and motion trajectories for different subgroups are represented by circles and curves with various colors.

decreasing spatial cohesion are presented. With the increasing size at the same critical distance, the average member distance grows slightly but the spatial cohesion decreases significantly, which is in accordance with empirical observations because large subgroups are more likely to be disintegrated into multiple small subgroups [42]. Consequently, the above results suggest that the critical distance can be regarded as a good representation of spatial cohesion, which is helpful for quantitatively describing the aggregation behavior of subgroup members.

B. Effect of Spatial Cohesion on Evacuation Processes

According to these findings in the previous section, we are interested in exploring the effect of spatial cohesion on evacuation processes. Here, an experimental room of $5m \times 5m$ with a single exit of $1.2m$ width from an empirical study [40] is chosen as the simulation scenario, and the initial positions of all pedestrians are limited to a square area of $3m \times 3m$ in the center of the experimental room. By adjusting different intensities of the spatial cohesion (i.e., critical distance $d_i^* = 0.5m$, $1.0m$, $1.5m$, and $2.0m$), subgroups with size $n_g = 2$, 4, 6, and 8 randomly generated in the initial area are designated to escape towards the exit, respectively. Similarly, we run 100 numerical simulations for each case to reduce accidental results, and the box plots of the overall evacuation time (i.e., the time consumed by all subgroup members to leave the experimental room) are shown in Fig. 4. At the same critical distance, a larger subgroup size implies a longer overall evacuation time, because the growing number of pedestrians near the exit is more likely to cause congestion and time delays. However, the overall evacuation time is prolonged as the critical distance increases regardless of the subgroup size. This indicates that a higher intensity of spatial cohesion has a certain promoting effect on the efficiency of subgroup evacuation, owing to the fact that the members behind will accelerate to keep a closer relative distance to the members in front to avoid falling behind.

Given the existence of diverse social relationships in real situations [43], this may give rise to the heterogeneous characteristics of spatial cohesion. For simplicity, without loss of generality, the critical distance is assumed to follow a uniform distribution $d_i^* \sim U(\tilde{d}_i^* - \sigma, \tilde{d}_i^* + \sigma)$, where $\tilde{d}_i^* = 1.2m$ stands for a moderate critical distance, and σ represents a heterogeneity coefficient that reflects the degree of

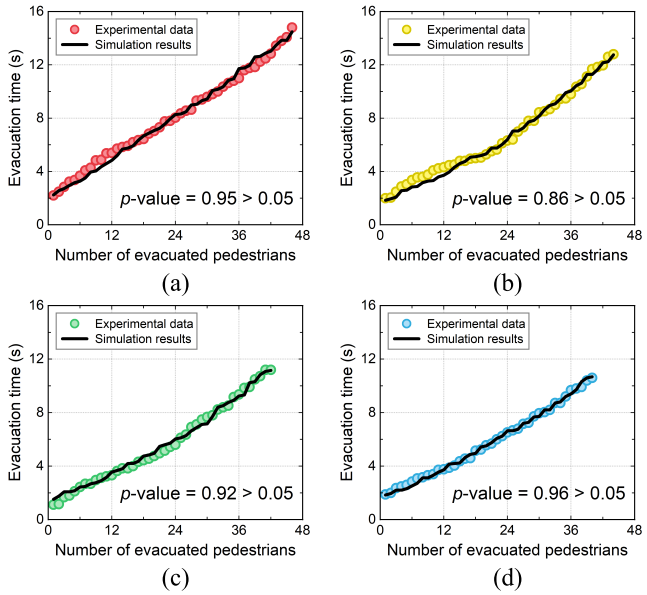

Fig. 7. Quantitative relationships between the evacuation time and the number of evacuated pedestrians. (a) $n_g = 2$. (b) $n_g = 4$. (c) $n_g = 6$. (d) $n_g = 8$. The experimental data and simulation results are represented by circles with various colors and black solid curves, respectively.

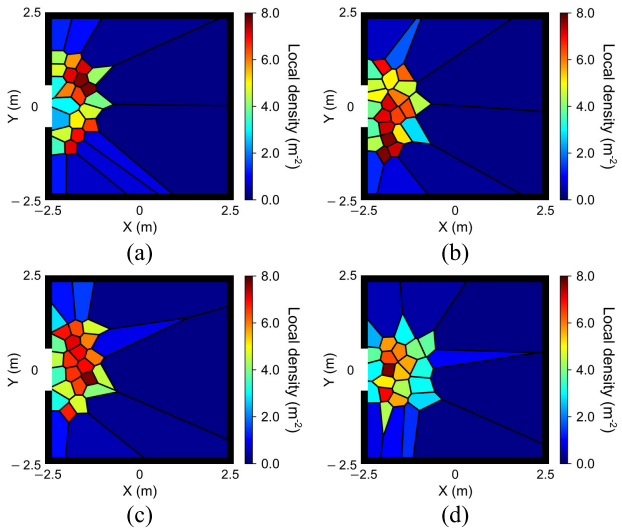

Fig. 8. Typical Voronoi density distributions under the fixed number of remaining pedestrians. (a) $n_g = 2$. (b) $n_g = 4$. (c) $n_g = 6$. (d) $n_g = 8$. The color coding within the Voronoi cell indicates the specific value of the local density.

differentiation. This stochasticity can be caused by inaccessible internal states of subgroup members at the initial time. We provide different values of the heterogeneity coefficient $\sigma = 0.2$, 0.4, 0.6, and 0.8, and simulate the escape behavior of subgroup members under the same conditions as other settings of the above simulation. To measure the motion characteristics of the entire evacuation process, the average subgroup speed is computed as $\bar{v}_g = \langle v_g(t) \rangle_t$, where $v_g(t) = \sum_{i \in g} \|\mathbf{v}_i(t)\| / n_g$ is the speed of subgroup g at time t. As illustrated in Fig. 5, the average subgroup speed presents a slightly decreasing tendency as the subgroup size increases, which has been revealed in field observations [12]. The impact of a greater heterogeneity coefficient σ on average subgroup speed is more significant for larger subgroup sizes, as reflected in broader longitudinal distributions. This confirms that the heterogeneity of spatial cohesion has a non-negligible effect on subgroup evacuation, which is also a key factor that needs to be considered for more realistic simulations of human collective behaviors.

C. Model Validation Based on an Empirical Study

This section is concerned with validating the reproducibility of our model via experimental data. First, we briefly introduce an empirical study conducted by Krüchten et al. on how subgroups influence evacuation dynamics [40], in which they organized a series of controlled experiments to allocate multiple participants for crowd evacuation in the previously mentioned scenario, and found that the evacuation time for larger subgroups is reduced due to the self-ordering effect. This work paves the way for model validation, where partial experimental groups used for data analysis (i.e., evacuation experiments in "GymBay" including crowds composed of subgroups with size $n_g = 2$, 4, 6, and 8, respectively) are selected to implement simulations. The model parameters are reasonably given for each case, and the initial positions of all pedestrians are guaranteed to correspond completely to the experimental conditions. The simulation snapshots of evacuation processes involving subgroups are clearly displayed in Fig. 6. It can be seen that the crowd consisting of larger subgroups evacuates more efficiently (i.e., fewer pedestrians remain in the scenario at the same time), which is a preliminary echo with the research findings under experimental conditions. We note that more individuals are forced to stick tightly to the wall on the exit side in numerical simulations, but this occurs less in experimental records. The reason might be that participants under experimental conditions are concerned about damaging the moveable artificial (not real) wall due to overcrowding.

We further analyze the quantitative relationship between the evacuation time and the number of evacuated pedestrians from the above simulation, and compare it with the records under experimental conditions. As shown in Fig. 7, the simulation results exhibit a fairly consistent tendency with the experimental data, and the Mann–Whitney–Wilcoxon U test confirms that there is almost no significant difference (p-value > 0.05), which indicates that the simulation results of our model are in accordance with empirical phenomena in terms of the temporal dimension. Moreover, we also verify the reproducibility of this model through the density distribution of crowd configuration. The Voronoi diagrams can be used to determine the local density at the position of each individual, which is inversely proportional to the area of the corresponding Voronoi cell [44]. The typical Voronoi density distributions are illustrated in Fig. 8 under the fixed number of remaining pedestrians (we set 30 pedestrians as an example here) for different simulation cases. It is apparent that the crowd surrounding the exit forms an "arch"-like configuration, which is elongated in the direction perpendicular to the exit for the case of larger subgroups. This reveals a self-ordering effect in larger subgroups that members prefer to order behind one another rather than next to each other, which reduces the number of conflicts triggered by individuals competing for space in front

TABLE II
PERFORMANCE EVALUATION OF VARIOUS SUBGROUP MODELS

Experimental group	Li et al. [15]		Xie et al. [17]		Moussaïd et al. [28]		Our model	
	MSE-ET	AHD-MT	MSE-ET	AHD-MT	MSE-ET	AHD-MT	MSE-ET	AHD-MT
Subgroup size = 2	3.717	0.624	1.318	0.617	0.848	0.558	**0.113**	**0.545**
Subgroup size = 4	2.202	0.590	1.216	0.762	0.449	0.645	**0.108**	**0.544**
Subgroup size = 6	1.643	0.965	0.675	1.102	0.240	0.769	**0.077**	**0.686**
Subgroup size = 8	0.720	0.980	0.393	1.121	0.293	0.552	**0.030**	**0.478**

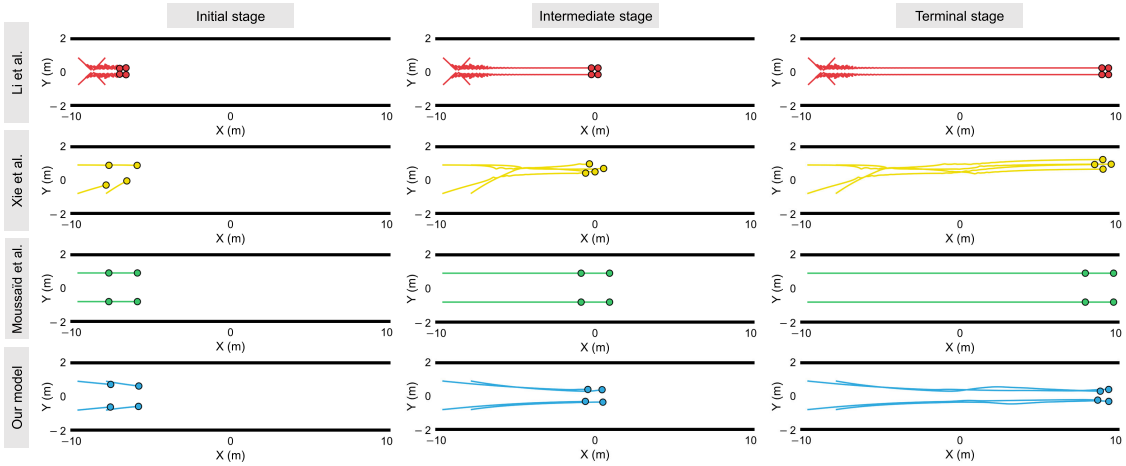

Fig. 9. Comparison of the aggregation behaviors under the condition of dispersed members. The vertical direction indicates different subgroup models, and the horizontal direction denotes the three stages of the movement process. The subgroup members and motion trajectories for different models are represented by circles and curves with various colors.

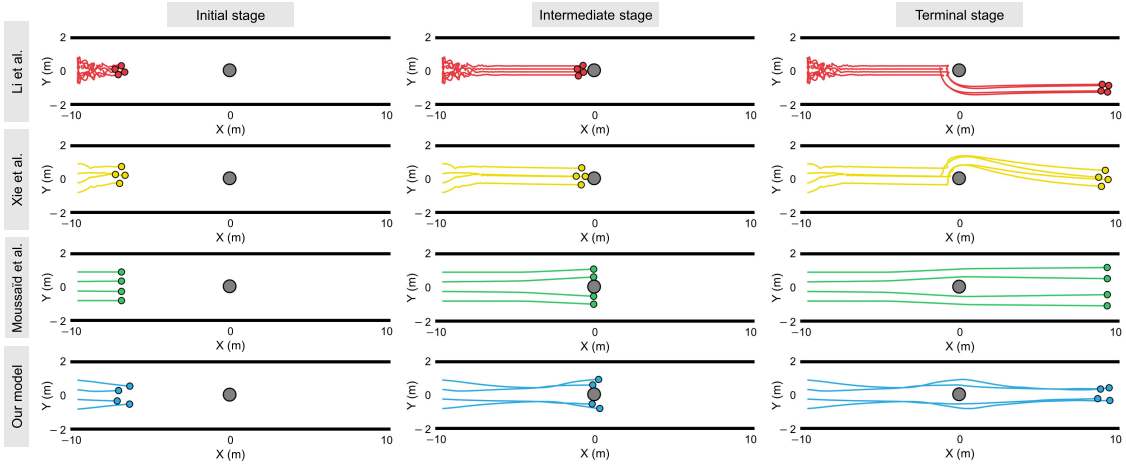

Fig. 10. Comparison of the avoidance behaviors under the condition of a static obstacle. The vertical direction indicates different subgroup models, and the horizontal direction denotes the three stages of the movement process. The subgroup members and motion trajectories for different models are represented by circles and curves with various colors. The gray circle in the middle of the walkway implies the static obstacle (e.g., cylinder).

of the exit. Therefore, it further confirms the validity of our model in reproducing empirical phenomena from the spatial dimension.

D. Performance Comparison With Existing Models

In the last section of numerical simulations, it is necessary to compare our model with existing models to highlight its superiority. For this, three representative subgroup models are selected as follows: The first two were proposed by Li et al. [15] (i.e., introducing the attraction among subgroup members into the SFM) and Xie et al. [17] (i.e., combining the long-range attraction and short-range repulsion among subgroup members into the SFM). The latter one was developed by Moussaïd et al. [28] (i.e., integrating two heuristic rules for individual movement into a force-based model). To begin with, we design three interaction contexts in a walkway scenario of $20m \times 4m$, which include the aggregation behaviors among dispersed members, avoidance behaviors in the face of a static obstacle, and avoidance behaviors in the face of a dynamic obstacle, respectively. With the initial conditions of all pedestrians guaranteed to be identical, we program and simulate subgroup behaviors based on the equations and parameters given in these models, and qualitatively compare them with the simulation effects of our model.

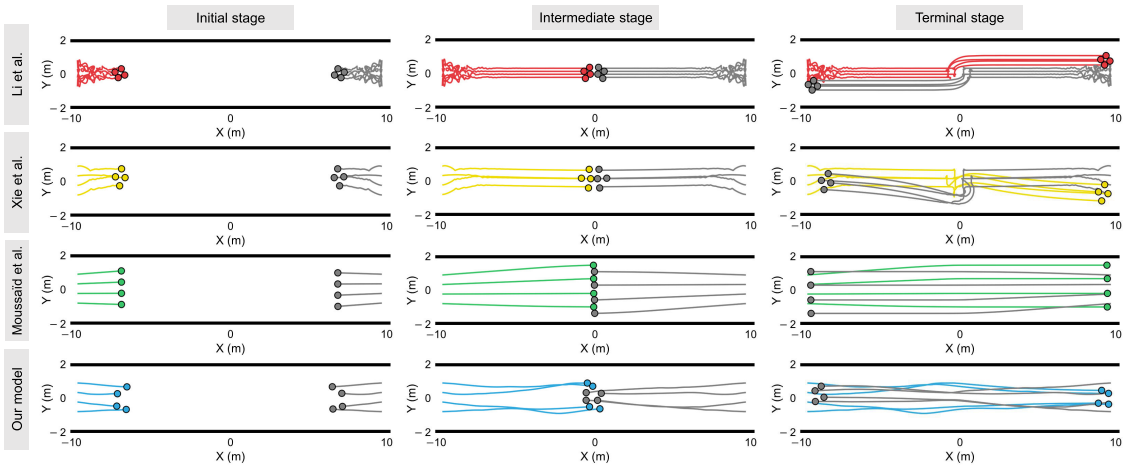

Fig. 11. Comparison of the avoidance behaviors under the condition of a dynamic obstacle. The vertical direction indicates different subgroup models, and the horizontal direction denotes the three stages of the movement process. The subgroup members and motion trajectories for different models are represented by circles and curves with various colors. The gray circles on the right side of the walkway imply the dynamic obstacle (e.g., another oncoming subgroup).

First, the aggregation behaviors simulated by these models are shown in Fig. 9, in which four dispersed subgroup members aim to move towards the other side of the walkway in an aggregated form. In terms of Li et al.'s model, the aggregation of subgroup members in the initial stage produces unrealistic back-and-forth oscillations. Although Xie et al.'s model forms a relatively natural aggregation process, it requires an explicitly designated leader (which may not necessarily exist in real situations). Even if Moussaïd et al.'s model contains visual avoidance, it is still difficult to achieve the aggregation of members due to the lack of cohesion effects. On the contrary, only our model can display the aggregation behavior of dispersed members that is more consistent with human subjective perception. Then, the avoidance behaviors when subgroup members face a static obstacle in the middle of the walkway are presented in Fig. 10. It is obvious that Li et al.'s and Xie et al.'s models do not consider the visual perception of individuals, resulting in illogical collisions between the subgroup with the static obstacle and eventually reaching the other side of the walkway in a forced twist. Although Moussaïd et al.'s model can generate effective avoidance behavior, these subgroup members are unable to reaggregate after the intermediate stage. However, our model realizes a smooth process of the subgroup first splitting and then merging, in good agreement with the avoidance behavior in real situations [45]. Last, two oncoming subgroups (i.e., facing a dynamic obstacle) in Fig. 11 also exhibit similar avoidance behavior, in which one splits to the two sides and the other gathers towards the middle when they are interacting. In other words, the avoidance interactions simulated by Li et al.'s and Xie et al.'s models are grossly inconsistent with empirical observations due to the neglect of visual perception, while Moussaïd et al.'s model is not capable of aggregating subgroup members with each other. Overall, our model can compensate for the essential deficiencies of these models, which leads to more natural and realistic subgroup behaviors.

To go beyond a purely qualitative analysis, we also quantitatively compare the reproduction effects of these models based on experimental datasets [40]. For this, two evaluation metrics are defined to quantify the similarity between the simulation results and the experimental data from the temporal and spatial dimensions. One is the mean squared error of evacuation times (MSE-ET), and another is the average Hausdroff distance of movement trajectories (AHD-MT). Note that the reproduction effects will be better if both MSE-ET and AHD-MT are closer to zero. For experimental groups of different subgroup sizes, Table II presents the performance evaluation of various subgroup models. The MSE-ET indicates that the evacuation times of pedestrians simulated by our model are almost significantly consistent with the experimental data. The AHD-MT shows that the simulation results from all subgroup models have inevitable deviations, because it is very hard to reproduce the uncertainty of individual movement in real situations. Nevertheless, our model still performs better compared to other existing models. In summary, these results further demonstrate the superiority of our model from a quantitative perspective.

IV. Conclusion

In this paper, we develop an interpretable model to simulate subgroup behaviors during evacuation. On the basis of quantifying individual visual information, the mechanisms of avoidance with the environment and attraction to other members within the field of view are explicitly clarified. We define two cognitive heuristics to determine the desired directions and desired speeds of subgroup members, and incorporate them into the nonlinear equations of motion. By conducting numerical simulations, several key conclusions are summarized as follows: (1) The critical distance to avoid separation reveals the spatial characteristics of subgroup members, which can essentially be viewed as a good representation of spatial cohesion. (2) A higher intensity of spatial cohesion has a more significant promotion to the efficiency of subgroup evacuation, and a greater heterogeneity of spatial cohesion reflects a larger variation in average subgroup speed. (3) Our model presents the simulation results fairly consistent with the experimental data from an empirical study, and its reproducibility has been validated from the temporal and spatial dimensions. (4) By comparing with existing models from both qualitative and quantitative perspectives, our model shows the dual advantage

of both visual avoidance and cohesion effect, as well as better performance in reproduction effects.

This work is beneficial to facilitate the understanding of subgroup behaviors in emergency situations and establish evacuation strategies tallying with realistic implications. On the one hand, many interesting laws of subgroups have been found to exist under normal conditions. Here are several examples, the number of subgroups decreases sharply with increasing size, approximately following a (truncated) Poisson distribution [46]. As crowd density changes from low to high, the spatial configurations of subgroups exhibit side-by-side, "V"-like or "U"-like [32], and "river"-like [47] formations in turn. However, the unpredictability of disasters and accidents results in a serious lack of data to study the phenomena and behaviors of subgroups in emergency situations, making computer simulations a potential research tool. In this case, the proposed model is expected to provide an effective solution for subgroup research. On the other hand, our simulation results may pave the way for more targeted guidance on crowd evacuation. Owing to the diversity of environmental characteristics (e.g., risk level, building layout, and incident type) and subgroup characteristics (e.g., proportion, size, and social relationships) [13], researchers have the flexibility to create a variety of scenarios and set subgroup-related parameters for numerical simulations, and contribute valuable insights to crowd evacuation by related methods such as optimizing the building layout and developing faster escape routes.

It is worth noting that the limitations of our model also need to be emphasized. First, it is feasible to assume that the line of sight is the same as the actual movement direction, but it must acknowledge the fact that individuals may experience head rotations and change the line of sight due to the influence of their surrounding environments [48]. However, this factor is difficult to be introduced into our model because it has great uncertainty and will extremely exacerbate the computational complexity. Second, to simplify the modeling process, it is supposed that vision is the only source for individuals to acquire external information, but human senses (e.g., audition, olfaction, and tactility) are more abundant in reality [49], and the corresponding information can be used as additional factors to be included in subsequent improved models. Despite its limitations, this model certainly helps us to better realize the behavioral characteristics of subgroups during evacuation, and relevant findings may also be applied to other fields such as multimode process control in industrial systems [50], [51] and collective decision making in swarm robotics [52], [53]. In summary, we hope that this work will bring inspiration for constructing more precise human collective motion models, which is of great significance for crowd management during large-scale events in the future.

REFERENCES

[1] G. Sreenu and M. A. Saleem Durai, "Intelligent video surveillance: A review through deep learning techniques for crowd analysis," *J. Big Data*, vol. 6, no. 1, p. 48, Dec. 2019.

[2] S. Yang, T. Li, X. Gong, B. Peng, and J. Hu, "A review on crowd simulation and modeling," *Graph. Models*, vol. 111, Sep. 2020, Art. no. 101081.

[3] J. Gao, Y. Yuan, and Q. Wang, "Feature-aware adaptation and density alignment for crowd counting in video surveillance," *IEEE Trans. Cybern.*, vol. 51, no. 10, pp. 4822–4833, Oct. 2021.

[4] J. Gao, T. Han, Y. Yuan, and Q. Wang, "Domain-adaptive crowd counting via high-quality image translation and density reconstruction," *IEEE Trans. Neural Netw. Learn. Syst.*, vol. 34, no. 8, pp. 4803–4815, Aug. 2023.

[5] Y. Zhou, B. P. L. Lau, Z. Koh, C. Yuen, and B. K. K. Ng, "Understanding crowd behaviors in a social event by passive WiFi sensing and data mining," *IEEE Internet Things J.*, vol. 7, no. 5, pp. 4442–4454, May 2020.

[6] K. Gkountakos, K. Ioannidis, T. Tsikrika, S. Vrochidis, and I. Kompatsiaris, "A crowd analysis framework for detecting violence scenes," in *Proc. Int. Conf. Multimedia Retr.*, Jun. 2020, pp. 276–280.

[7] P. Kothari, S. Kreiss, and A. Alahi, "Human trajectory forecasting in crowds: A deep learning perspective," *IEEE Trans. Intell. Transp. Syst.*, vol. 23, no. 7, pp. 7386–7400, Jul. 2022.

[8] Q. Tang, F. Liu, J. Jiang, and Y. Zhang, "EPRNet: Efficient pyramid representation network for real-time street scene segmentation," *IEEE Trans. Intell. Transp. Syst.*, vol. 23, no. 7, pp. 7008–7016, Jul. 2022.

[9] X. Zheng, T. Zhong, and M. Liu, "Modeling crowd evacuation of a building based on seven methodological approaches," *Building Environ.*, vol. 44, no. 3, pp. 437–445, Mar. 2009.

[10] H. Vermuyten, J. Beliën, L. De Boeck, G. Reniers, and T. Wauters, "A review of optimisation models for pedestrian evacuation and design problems," *Saf. Sci.*, vol. 87, pp. 167–178, Aug. 2016.

[11] D. Helbing and A. Johansson, "Pedestrian, crowd and evacuation dynamics," in *Encyclopedia of Complexity and Systems Science*. Cham, Switzerland: Springer, 2009, pp. 6476–6495.

[12] A. Nicolas and F. H. Hassan, "Social groups in pedestrian crowds: Review of their influence on the dynamics and their modelling," *Transportmetrica A, Transp. Sci.*, vol. 19, no. 1, Jan. 2023, Art. no. 1970651.

[13] W. Wu and X. Zheng, "A systematic analysis of subgroup research in pedestrian and evacuation dynamics," *IEEE Trans. Intell. Transp. Syst.*, vol. 25, no. 2, pp. 1225–1246, Feb. 2024.

[14] D. Helbing, I. Farkas, and T. Vicsek, "Simulating dynamical features of escape panic," *Nature*, vol. 407, no. 6803, pp. 487–490, Sep. 2000.

[15] Y. Li, H. Liu, G.-P. Liu, L. Li, P. Moore, and B. Hu, "A grouping method based on grid density and relationship for crowd evacuation simulation," *Phys. A, Stat. Mech. Appl.*, vol. 473, pp. 319–336, May 2017.

[16] H. Zhang, H. Liu, X. Qin, and B. Liu, "Modified two-layer social force model for emergency earthquake evacuation," *Phys. A, Stat. Mech. Appl.*, vol. 492, pp. 1107–1119, Feb. 2018.

[17] W. Xie, E. W. M. Lee, T. Li, M. Shi, R. Cao, and Y. Zhang, "A study of group effects in pedestrian crowd evacuation: Experiments, modelling and simulation," *Saf. Sci.*, vol. 133, Jan. 2021, Art. no. 105029.

[18] H. Strasburger, "Seven myths on crowding and peripheral vision," *I-Perception*, vol. 11, no. 3, May 2020, Art. no. 204166952091305.

[19] R. Bastien and P. Romanczuk, "A model of collective behavior based purely on vision," *Sci. Adv.*, vol. 6, no. 6, Feb. 2020, Art. no. eaay0792, doi: 10.1126/sciadv.aay0792.

[20] R. Sarfati, J. C. Hayes, and O. Peleg, "self-organization in natural swarms of *Photinus carolinus* synchronous fireflies," *Sci. Adv.*, vol. 7, no. 28, Jul. 2021, Art. no. eabg9259, doi: 10.1126/sciadv.abg9259.

[21] A. Strandburg-Peshkin et al., "Visual sensory networks and effective information transfer in animal groups," *Current Biol.*, vol. 23, no. 17, pp. R709–R711, Sep. 2013.

[22] S. B. Rosenthal, C. R. Twomey, A. T. Hartnett, H. S. Wu, and I. D. Couzin, "Revealing the hidden networks of interaction in mobile animal groups allows prediction of complex behavioral contagion," *Proc. Nat. Acad. Sci. USA*, vol. 112, no. 15, pp. 4690–4695, Mar. 2015.

[23] M. Ballerini, "Interaction ruling animal collective behavior depends on topological rather than metric distance: Evidence from a field study," *Proc. Nat. Acad. Sci. USA*, vol. 105, no. 4, pp. 1232–1237, 2008.

[24] D. J. G. Pearce, A. M. Miller, G. Rowlands, and M. S. Turner, "Role of projection in the control of bird flocks," *Proc. Nat. Acad. Sci. USA*, vol. 111, no. 29, pp. 10422–10426, Jul. 2014.

[25] B. H. Lemasson, J. J. Anderson, and R. A. Goodwin, "Collective motion in animal groups from a neurobiological perspective: The adaptive benefits of dynamic sensory loads and selective attention," *J. Theor. Biol.*, vol. 261, no. 4, pp. 501–510, Dec. 2009.

[26] T. Vicsek and A. Zafeiris, "Collective motion," *Phys. Rep.*, vol. 517, no. 3, pp. 71–140, 2012.

[27] D. Helbing, I. J. Farkas, P. Molnar, and T. Vicsek, "Simulation of pedestrian crowds in normal and evacuation situations," in *Pedestrian and Evacuation Dynamics*, vol. 21. Cham, Switzerland: Springer, 2002, pp. 21–58.

[28] M. Moussaïd, D. Helbing, and G. Theraulaz, "How simple rules determine pedestrian behavior and crowd disasters," *Proc. Nat. Acad. Sci. USA*, vol. 108, no. 17, pp. 6884–6888, 2011.

[29] Y. Ma, E. W. M. Lee, and M. Shi, "Dual effects of guide-based guidance on pedestrian evacuation," *Phys. Lett. A*, vol. 381, no. 22, pp. 1837–1844, Jun. 2017.

[30] Q. Meng, M. Zhou, J. Liu, and H. Dong, "Pedestrian evacuation with herding behavior in the view-limited condition," *IEEE Trans. Computat. Social Syst.*, vol. 6, no. 3, pp. 567–575, Jun. 2019.

[31] W. Yi, W. Wu, J. Li, X. Wang, and X. Zheng, "An extended queueing model based on vision and morality for crowd evacuation," *Phys. A, Stat. Mech. Appl.*, vol. 604, Oct. 2022, Art. no. 127658.

[32] M. Moussaïd, N. Perozo, S. Garnier, D. Helbing, and G. Theraulaz, "The walking behaviour of pedestrian social groups and its impact on crowd dynamics," *PLoS One*, vol. 5, no. 4, Apr. 2010, Art. no. e10047.

[33] P. R. Schrater, D. C. Knill, and E. P. Simoncelli, "Mechanisms of visual motion detection," *Nature Neurosci.*, vol. 3, no. 1, pp. 64–68, Jan. 2000.

[34] J. Bill, S. J. Gershman, and J. Drugowitsch, "Visual motion perception as online hierarchical inference," *Nature Commun.*, vol. 13, no. 1, p. 7403, Dec. 2022.

[35] G. Gigerenzer, "Why heuristics work," *Perspect. Psychol. Sci.*, vol. 3, no. 1, pp. 20–29, Jan. 2008.

[36] A. Turner and A. Penn, "Encoding natural movement as an agent-based system: An investigation into human pedestrian behaviour in the built environment," *Environ. Planning B, Planning Design*, vol. 29, no. 4, pp. 473–490, Aug. 2002.

[37] I. D. Couzin, J. Krause, N. R. Franks, and S. A. Levin, "Effective leadership and decision-making in animal groups on the move," *Nature*, vol. 433, no. 7025, pp. 513–516, Feb. 2005.

[38] D. Strömbom, "Collective motion from local attraction," *J. Theor. Biol.*, vol. 283, no. 1, pp. 145–151, Aug. 2011.

[39] L. Fu, S. Cao, Y. Shi, S. Chen, P. Yang, and J. Fang, "Walking behavior of pedestrian social groups on stairs: A field study," *Saf. Sci.*, vol. 117, pp. 447–457, Aug. 2019.

[40] C. von Krüchten and A. Schadschneider, "Empirical study on social groups in pedestrian evacuation dynamics," *Phys. A, Stat. Mech. Appl.*, vol. 475, pp. 129–141, Jun. 2017.

[41] J. E. Herbert-Read, A. Perna, R. P. Mann, T. M. Schaerf, D. J. T. Sumpter, and A. J. W. Ward, "Inferring the rules of interaction of shoaling fish," *Proc. Nat. Acad. Sci. USA*, vol. 108, no. 46, pp. 18726–18731, Nov. 2011.

[42] V. Reuter, B. S. Bergner, G. Köster, M. Seitz, F. Treml, and D. Hartmann, "On modeling groups in crowds: Empirical evidence and simulation results including large groups," in *Pedestrian and Evacuation Dynamics 2012*. Cham, Switzerland: Springer, 2013, pp. 835–845.

[43] Z. Yucel, F. Zanlungo, C. Feliciani, A. Gregorj, and T. Kanda, "Identification of social relation within pedestrian dyads," *PLoS One*, vol. 14, no. 10, Oct. 2019, Art. no. e0223656.

[44] B. Steffen and A. Seyfried, "Methods for measuring pedestrian density, flow, speed and direction with minimal scatter," *Phys. A, Stat. Mech. Appl.*, vol. 389, no. 9, pp. 1902–1910, May 2010.

[45] H. Singh, R. Arter, L. Dodd, P. Langston, E. Lester, and J. Drury, "Modelling subgroup behaviour in crowd dynamics DEM simulation," *Appl. Math. Model.*, vol. 33, no. 12, pp. 4408–4423, Dec. 2009.

[46] W. Wu, W. Yi, X. Wang, and X. Zheng, "A force-based model for adaptively controlling the spatial configuration of pedestrian subgroups at non-extreme densities," *Transp. Res. Part C, Emerg. Technol.*, vol. 152, Jul. 2023, Art. no. 104154.

[47] D. Helbing, L. Buzna, A. Johansson, and T. Werner, "Self-organized pedestrian crowd dynamics: Experiments, simulations, and design solutions," *Transp. Sci.*, vol. 39, no. 1, pp. 1–24, Feb. 2005.

[48] E. Murphy-Chutorian and M. M. Trivedi, "Head pose estimation in computer vision: A survey," *IEEE Trans. Pattern Anal. Mach. Intell.*, vol. 31, no. 4, pp. 607–626, Apr. 2009.

[49] I. Knez, J. Willander, A. Butler, Å. O. Sang, I. Sarlöv-Herlin, and A. Åkerskog, "I can still see, hear and smell the fire: Cognitive, emotional and personal consequences of a natural disaster, and the impact of evacuation," *J. Environ. Psychol.*, vol. 74, Apr. 2021, Art. no. 101554.

[50] K. Huang, K. Wei, F. Li, C. Yang, and W. Gui, "LSTM-MPC: A deep learning based predictive control method for multimode process control," *IEEE Trans. Ind. Electron.*, vol. 70, no. 11, pp. 11544–11554, Nov. 2023.

[51] K. Huang et al., "Adaptive multimode process monitoring based on mode-matching and similarity-preserving dictionary learning," *IEEE Trans. Cybern.*, vol. 53, no. 6, pp. 3974–3987, Jun. 2023.

[52] J. F. Boudet et al., "From collections of independent, mindless robots to flexible, mobile, and directional superstructures," *Sci. Robot.*, vol. 6, no. 56, Jul. 2021, Art. no. eabd0272, doi: 10.1126/scirobotics.abd0272. [Online]. Available: https://www.science.org/doi/abs/10.1126/scirobotics.abd0272

[53] M. Dorigo, G. Theraulaz, and V. Trianni, "Swarm robotics: Past, present, and future [point of view]," *Proc. IEEE*, vol. 109, no. 7, pp. 1152–1165, Jul. 2021.

Wenhan Wu received the B.S. degree from the School of Automation, Central South University, Changsha, China, in 2019. He is currently pursuing the Ph.D. degree in control science and engineering with the Department of Automation, Tsinghua University, Beijing, China. From April 2023 to April 2024, he was a joint Ph.D. Student at the Institute for Theoretical Biology, Department of Biology, Humboldt Universität zu Berlin, Berlin, Germany. His current research interests include collective behavior, emergency evacuation, pedestrian group, network science, and decision making.

Wenfeng Yi received the B.S. degree from the School of Astronautics, Beihang University, Beijing, China, in 2019. He is currently pursuing the Ph.D. degree in control science and engineering with the Department of Automation, Tsinghua University, Beijing. From November 2023 to May 2024, he was a joint Ph.D. Student with the School of Biological Sciences, University of Bristol, Bristol, U.K. His current research interests include collective behavior, emergency evacuation, pedestrian queueing, and swarm robotics.

Xiaolu Wang received the Ph.D. degree in control theory and control engineering from Beijing University of Chemical Technology in 2015. She is currently an Assistant Researcher with the Department of Automation, Tsinghua University, Beijing, China. Her current research interests include crowd evacuation intervention mechanism, evacuation dynamics, and emergency management.

Xiaoping Zheng received the B.S. degree from Chengdu University of TCM, Chengdu, China, in 1995, and the Ph.D. degree from Sichuan University, Chengdu, in 2003.

From 2004 to 2006, he was a Post-Doctoral Researcher with the School of Management, Fudan University, Shanghai, China. From 2006 to 2013, he was a Professor with the Institute of Safety Management, Beijing University of Chemical Technology, Beijing, China. He is currently a Professor with the Department of Automation, Tsinghua University, Beijing. He was a 973 Chief Scientist in 2011. He was a recipient of the National Science Fund for Distinguished Young Scholars in 2012 and a Distinguished Professor of the Chang Jiang Scholars Program in 2021. His current research interests include large-scale crowd evacuation, evolutionary game theory, and terahertz technology.